

Dynamical localization and slow dynamics in quasiperiodically-driven quantum systems

Vatsana Tiwari,¹ Devendra Singh Bhakuni,² and Auditya Sharma^{1,*}

¹*Department of Physics, Indian Institute of Science Education and Research, Bhopal, India*

²*Department of Physics, Ben-Gurion University of the Negev, Beer-Sheva 84105, Israel*

We investigate the role of a quasiperiodically driven electric field in a one-dimensional disordered fermionic chain. In the clean non-interacting case, we show the emergence of dynamical localization - a phenomenon previously known to exist only for a perfect periodic drive. In contrast, in the presence of disorder, where a periodic drive preserves Anderson localization, we show that the quasiperiodic drive destroys it and leads to slow relaxation. Considering the role of interactions, we uncover the phenomenon of *quasiperiodic driving-induced logarithmic relaxation*, where a suitably tuned drive (corresponding to dynamical localization in the clean, non-interacting limit) slows down the dynamics even when the disorder is small enough for the system to be in the ergodic phase. This is in sharp contrast to the fast relaxation seen in the undriven model, as well as the absence of thermalization (drive-induced MBL) exhibited by a periodically driven model.

Introduction: The non-equilibrium properties of a quantum system subjected to a time-dependent drive have been a topic of great interest [1–4]. Driven systems exhibit many exciting and counter-intuitive features absent in their undriven counterparts. Notable examples of such striking phenomena in periodically driven systems include dynamical localization in kicked rotors [5–7], dynamical freezing [8], Floquet topological insulators [9, 10], Floquet prethermalization [11–15] and Floquet time crystals [16–19]. A specific class of time-periodically driven systems is one with an *electric-field drive* that results in a variety of interesting phenomena such as dynamical localization [20–24], coherent destruction of Wannier Stark localization [22, 25–28], and super Bloch oscillations [22, 27–30]. The inclusion of many-body interactions, further opens up fascinating possibilities such as Stark-many body localization [31–39], drive-induced many-body localization [28, 40], and Stark time crystals [41, 42]. An important question is whether such features still arise in the absence of a perfect time-periodicity of the drive.

While an enormous body of work has been devoted to periodic drives, the exploration of the role of quasiperiodic driving has recently gained traction [43–55]. Features like prethermalization [48, 56], coherence restoration [57], and quasi-time crystals [45] are associated with such drives. Furthermore, experiments have realized dynamical phases employing quasiperiodic driving [58]. In this Letter, we explore the properties of a system driven by a *quasiperiodic electric field*. Specifically, we address the question of whether a quasiperiodic electric-field drive can give rise to dynamical localization, and if it does, what the effect of interactions and disorder on dynamical localization would be.

We address these questions by considering two discrete forms of quasiperiodic driving: Fibonacci and Thue-Morse [44, 49, 50]. For these sequences, we find that in the non-interacting limit, the phenomenon of dynamical localization occurs when the parameters of the drive are tuned appropriately. We derive the conditions under

Driving Protocol	$W = 0$ $U = 0$	$W \neq 0$ $U = 0$	$W \neq 0, U \neq 0$ <i>ergodic regime</i>
Undriven	Fast relaxation	Anderson localization[59]	Fast relaxation [60]
Periodic	Dynamic localization (Periodic oscillation) [20]	Anderson localization [26]	Drive-induced MBL [28]
Quasi-periodic	Dynamic localization (Periodic oscillation)	Slow relaxation $S(t) \propto t^\gamma$, $\gamma < 1$	Drive-induced logarithmic relaxation $S(t) \propto \log t$

Table I. Schematic of the main results for the quasiperiodic drive and a comparison with existing results for the periodic and undriven cases. The third row contains the central findings of our work. The table is constructed by analyzing the auto-correlation function (Eq. 10) and entanglement entropy (Eq. 9).

which dynamical localization is realized and numerically demonstrate this by studying the dynamics of return probability and entanglement entropy. In the presence of disorder, where the undriven system exhibits Anderson localization [59, 61], we find that the quasiperiodic drive destroys Anderson localization and leads to a slow relaxation of the return probability together with a *sub-linear* growth of entanglement entropy irrespective of the tuning of drive parameters.

Interestingly, many-body interactions applied to the clean system destroy dynamical localization, and the system approaches an infinite-temperature-like state. However, this approach to an infinite-temperature-like state is relatively slow if the parameters are tuned at the dynamical localization point as opposed to any arbitrary choices of the parameters. This follows from the fact that the drive suppresses the hopping parameters significantly at the dynamical localization point. Next, we demonstrate how the hopping suppression can be ex-

exploited to manipulate the dynamical behavior of a disordered many-body interacting system. Starting from the ergodic phase in the weak disorder limit of the undriven model, where the auto-correlation function is known to exhibit power-law decay accompanied by diffusive transport with a disorder-dependent dynamical exponent [60], we show that a quasiperiodic electric-field drive can in fact lead to a slow logarithmic relaxation. This is in sharp contrast to the periodic case, where the drive is known to give rise to drive-induced many-body localization [40]. In Table (I), the chief findings from our work are summarized alongside already established results in the literature.

Model Hamiltonian and driving protocol: We consider a disordered interacting one-dimensional tight-binding chain subjected to a time-dependent electric field. The model Hamiltonian can be written as:

$$H = -\frac{\Delta}{4} \sum_{j=0}^{L-2} \left(c_j^\dagger c_{j+1} + h.c. \right) + \mathcal{F}(t) \sum_{j=0}^{L-1} j \left(n_j - \frac{1}{2} \right) + \sum_{j=0}^{L-1} h_j \left(n_j - \frac{1}{2} \right) + U \sum_{j=0}^{L-2} \left(n_j - \frac{1}{2} \right) \left(n_{j+1} - \frac{1}{2} \right), \quad (1)$$

where c_j and c_j^\dagger are fermionic annihilation and creation operators respectively, n_j are number operators, Δ is the hopping strength, U is the strength of nearest-neighbor interaction, and h_j is the on-site potential which is taken to be a random number drawn from a box distribution: $h_j \in [-W, W]$. For the undriven case ($\mathcal{F}(t) = 0$), Eqn. 1 is the standard model of many-body localization (MBL) where a transition from an ergodic phase to a many-body localized phase occurs on varying the disorder strength [62, 63], although the precise value of the critical disorder strength is still controversial [64–66]. In this work, we focus only on the ergodic side of the MBL transition. The chain is subjected to a time-dependent field $\mathcal{F}(t)$. For a periodic drive with time period T : $\mathcal{F}(t+T) = \mathcal{F}(t)$, the clean non-interacting limit ($W = 0, U = 0$) exhibits dynamic localization for some specific choices of the driving amplitude and the frequency [20–24], while for a randomly fluctuating field there is no dynamical localization [27]. In this work, we focus on the case where the time-dependent field is neither periodic nor random but is rather quasiperiodic in nature and contains many frequencies in the Fourier spectrum. Our quasiperiodic driving protocols employ Fibonacci and Thue-Morse sequences [44, 49, 50].

For the Fibonacci sequence, we start by considering the unitary operators $U_0 = e^{-iTH_A}$ and $U_1 = e^{-iTH_B}$ where H_A and H_B are the Hamiltonians corresponding to the electric field $\mathcal{F}(t) = \pm F$ respectively (Eq. (1)) and generate the subsequent evolution according to the Fibonacci sequence [50]:

$$U_n = U_{n-2}U_{n-1}, \quad n \geq 2. \quad (2)$$

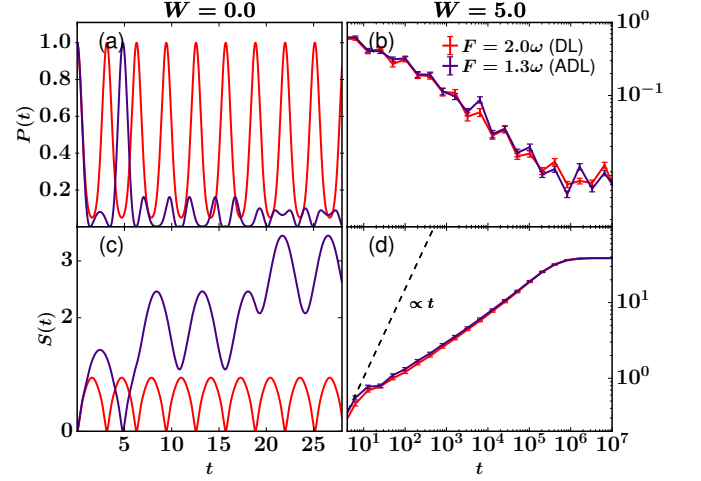


Figure 1. Dynamics of (a,b): return probability $P(t)$ and (c,d): entanglement entropy, for a Thue-Morse driven clean ($W = 0.0$) and disordered ($W = 5.0$) system. Data corresponding to a tuning of parameters both at dynamical localization (DL) ($F = \frac{n}{2}\omega$) and away from dynamical localization (ADL) ($F \neq n\omega$) are shown. The other parameters are $\Delta = 4.0, \omega = 1.0, L = 200$. For our numerics, we take the time discretization to be $\Delta t = 0.001$. For the disordered cases, we have averaged over 100 realizations of disorder. The (linear) black dashed line indicates the ballistic growth of entanglement entropy ($S(t) \propto t$).

The Thue-Morse sequence (TMS), on the other hand, can be generated using the recurrence relation [48]

$$U_{n+1} = \tilde{U}_n U_n, \quad \tilde{U}_{n+1} = U_n \tilde{U}_n, \quad (3)$$

where we start with the unitary operators $U_1 = U_B U_A$, $\tilde{U}_1 = U_A U_B$ with $U_B = e^{-iTH_B}$, and $U_A = e^{-iTH_A}$. The time evolution of the initial wave function can be then expressed as: $|\psi_n\rangle = U_n |\psi(0)\rangle$. This recursive construction enables us to simulate the dynamics for an exponentially long time with the aid of just a linearly increasing number of matrix multiplications for both Fibonacci and Thue-Morse driving [48].

Dynamical localization: We first consider the clean non-interacting limit ($W = 0, U = 0$). In this case, the Hamiltonian (1) can be written in terms of the unitary operators: [67] $\hat{K} = \sum_{n=-\infty}^{\infty} |n\rangle\langle n+1|$, $\hat{K}^\dagger = \sum_{n=-\infty}^{\infty} |n+1\rangle\langle n|$, and $\hat{N} = \sum_{n=-\infty}^{\infty} n |n\rangle\langle n|$, as

$$\hat{H} = -\frac{\Delta}{4} \left(\hat{K} + \hat{K}^\dagger \right) + \mathcal{F}(t) \hat{N}. \quad (4)$$

These operators follow the commutation relations:

$$[\hat{K}, \hat{N}] = \hat{K}, \quad [\hat{K}^\dagger, \hat{N}] = -\hat{K}^\dagger, \quad [\hat{K}, \hat{K}^\dagger] = 0. \quad (5)$$

With this form of the Hamiltonian and the commutation relations, we can write down the approximate effective Hamiltonian for Thue-Morse driving. We work out an

expression for the stroboscopic unitary operator defined at the m^{th} Thue-Morse level: $U(N = 2^m)$. With the aid of Eq. (3), we can express $U(N = 2^m)$ as a product of a string of Floquet unitary operators U_A and U_B . Using the BCH formula [68],

$$e^X e^Y = \exp \left[X + Y + \frac{1}{2} [X, Y] + \dots \right], \quad (6)$$

we can write $U(N = 2^m)$ in terms of an effective Hamiltonian H_{eff} (see supplementary section for details) as:

$$U(N = 2^m) \equiv \exp(-i2^m T H_{\text{eff}}). \quad (7)$$

Here, H_{eff} is given by

$$H_{\text{eff}} \equiv \Delta_{\text{eff}} (\hat{K} + \hat{K}^\dagger), \quad \Delta_{\text{eff}} = -\frac{\Delta}{4} \left[\frac{\sin(2F\pi/\omega)}{(2F\pi/\omega)} \right] \quad (8)$$

where, $\omega = \frac{2\pi}{T}$. Thus we see from Eq. (8) that the coefficients of \hat{K} and \hat{K}^\dagger get renormalized. When the amplitude of the drive is tuned at $\frac{F}{\omega} = \frac{n}{2} (n \in \mathbb{Z})$, the effective hopping term vanishes and any state will return to its initial position after this time period. Hence the system remains dynamically localized for arbitrary time as long as the drive is appropriately tuned. A similar result also holds for Fibonacci driving as shown in the supplementary section.

We test these results with the aid of numerical simulations of the dynamics of return probability which measures the probability of finding a particle after any instance at an initially localized site n . It is defined as: $P(t) = |\langle \psi(0) | \psi(t) \rangle|^2$; in our study, we take the particle to be localized initially at site $n = L/2$. The dynamics of the return probability for the Thue-Morse driven system is plotted in Fig. 1(a). For the ratio $F/\omega = 2.0$, we find that the return probability has oscillatory behavior in the short time limit. We have checked using stroboscopic dynamics that it periodically returns to its original value of unity even for very long times. On the other hand, tuning the ratio at $F/\omega = 1.3$, we see that the return probability is vanishingly small.

A similar observation can be made when looking at the growth of entanglement entropy defined as [69]

$$S(t) = -\text{Tr}(\rho_{L/2} \log \rho_{L/2}), \quad (9)$$

where $\rho_{L/2} = \text{Tr}_{1 \leq i \leq L/2} \{ |\psi(t)\rangle \langle \psi(t)| \}$ is the reduced density matrix of half the chain obtained by tracing out the other half of the chain. For non-interacting systems, a computationally efficient method can be used to calculate the entanglement entropy for larger system sizes by focusing on the two-point correlation function [27, 70, 71]. We start with an initial Neel state $|\psi(0)\rangle = \prod_{i=1}^{L/2} \hat{c}_{2i}^\dagger |0\rangle$, and plot the dynamics of the entanglement entropy in Fig. 1(c). Again, for the parameter tuned at the dynamical localization point, we find oscillatory behavior, while away from it, the entanglement entropy starts to grow

in time. These observations confirm the analytical prediction that when the ratio F/ω is tuned properly, the system exhibits dynamical localization, while away from it, the system behaves as just a nearest-neighbor chain with renormalized hopping.

Finally, we comment on the possibility of dynamical localization for any sequence of random unitary operators [48]. While the system is delocalized when the electric field is randomly flipped at arbitrary times (white-noise) [27], dynamical localization can be engineered for any random sequence of unitary operators applied for an equal amount of time and with proper tuning of the parameters. This can be accomplished by a method similar to the above where a proper choice of the parameters can yield an effective unitary operator that is equal to the identity operator.

We now consider the disordered case, which leads to Anderson localization [59, 61] for any non-zero value of the disorder strength in the undriven case. We study the stroboscopic evolution of the return probability and the entanglement entropy for disorder strength $W = 5.0$. As can be seen from Fig. 1(b), there is no sign of either dynamical localization or Anderson localization. Instead, we observe that Thue-Morse driving leads to a slow decay of the return probability accompanied by a sub-linear growth of the entanglement entropy $S(t) \propto t^\gamma$ where $\gamma < 1$. This contrasts with the perfect periodic drive case, where Anderson localization remains stable [26, 72]. It is also worth mentioning that due to the presence of disorder, the point of dynamical localization here is no longer special, and for the parameters tuned both at and away from dynamical localization, we observe similar features (Fig. 1b and 1d).

Slow-heating and drive-induced logarithmic relaxation: Having discussed the emergence of dynamical localization under quasiperiodic driving, we now explore the interplay of many-body interactions in such systems. We employ exact diagonalization for a system of size $L = 16$ at half-filling. We focus on the dynamics of entanglement entropy defined in Eqn.9. For driven quantum systems, the entanglement entropy typically saturates to the Page value: $S_{\text{Page}} = \frac{1}{2}(L \ln 2 - 1)$ which corresponds to the infinite temperature state [73, 74]. Additionally, we consider the decay of the auto-correlation function starting from an initial Neel state. The auto-correlation function is defined as [45, 60, 75–77]

$$C(t) = 4 \langle \hat{S}_{L/2}^z(t) \hat{S}_{L/2}^z(0) \rangle, \quad (10)$$

where $\hat{S}_i^z = \hat{n}_i - \frac{1}{2}$. While in the localized phase, the auto-correlation function $C(t)$ saturates to a non-zero value, in the ergodic phase, it rapidly goes to zero [45].

We first observe that dynamical localization is destroyed in the presence of many-body interactions. However, for both Fibonacci and Thue-Morse driving (see supplementary section), the dynamics is found to be very

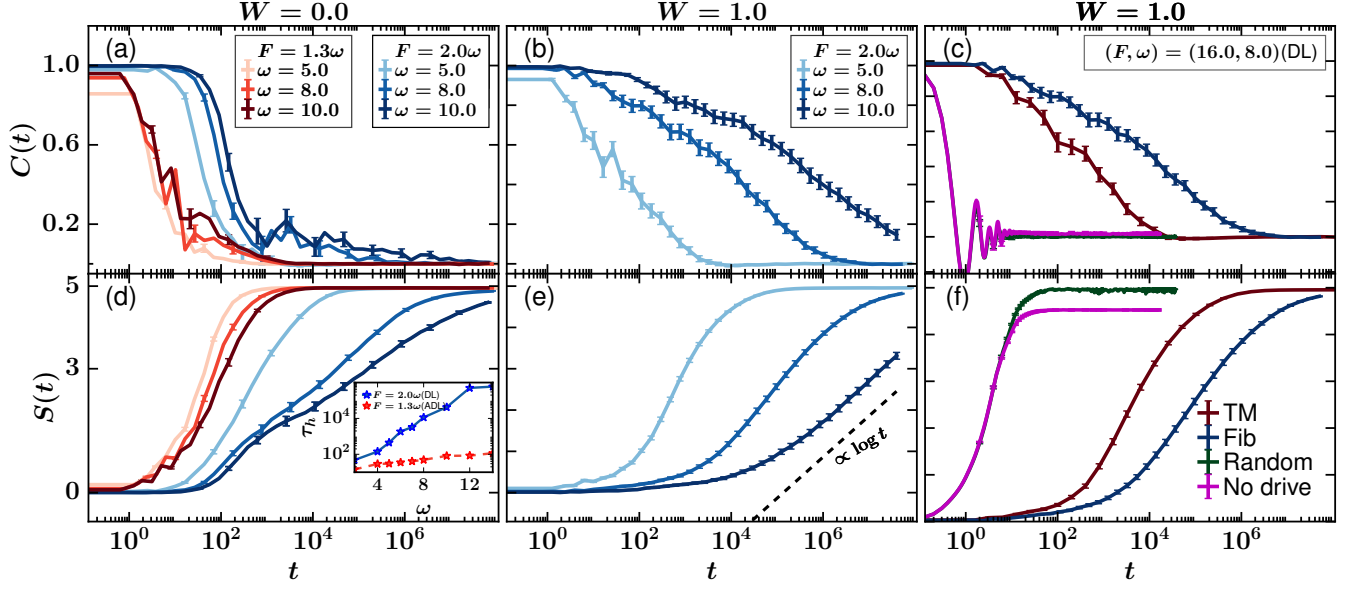


Figure 2. Dynamics of the auto-correlation function $C(t)$ and the half chain entanglement entropy $S(t)$ for the Fibonacci driven interacting fermionic system. (a, d): $C(t)$ and $S(t)$ for Fibonacci driven clean ($W = 0.0$) interacting system. The red shades correspond to a tuning of the parameters away from dynamical localization ($F = 1.3\omega$, ADL), and blue shades correspond to a tuning at dynamical localization ($F = 2.0\omega$, DL). Inset(d): Heating time τ_h as a function of frequency ω . (b, e): $C(t)$ and $S(t)$ for Fibonacci driven disordered ($W = 1.0$) interacting system. When disorder is present, we have averaged over 100 disorder realizations. (c, f): Comparison of dynamics of differently driven and undriven interacting disordered systems. In (e), the black dashed line shows logarithmic growth of entanglement entropy ($S(t) \propto \log t$) for $\omega = 10$. The other system parameters are $\Delta = 4.0$, $U = 1.0$, $F = 2.0\omega$, and system size $L = 16$.

slow if the interactions are turned on at the dynamical localization point as opposed to the case where the parameters are tuned away from it. Considering the clean limit ($W = 0$), in Fig. 2(a,d), we plot the dynamics of auto-correlation function $C(t)$, and entanglement entropy $S(t)$ for $\frac{F}{\omega} = 2$ (at DL) and $\frac{F}{\omega} = 1.3$ (away from DL) and a range of driving frequencies. We average the entanglement entropy and auto-correlation function over 50 different initial product states of the same energy density close to the Neel state. The entanglement entropy rapidly reaches the infinite-temperature Page value while the auto-correlation function quickly decays to zero for $\frac{F}{\omega} = 1.3$ for all the driving frequencies considered. On the other hand, for $\frac{F}{\omega} = 2$, the auto-correlation function exhibits a slow decay accompanied by a slow relaxation of the entanglement entropy to the Page value (Fig. 2(a,d)). On increasing the driving frequency, the growth further slows down, suggesting slow heating. To quantify the heating, we calculate the heating time τ_h defined as the time when the entanglement entropy attains half of the Page value [78]. The heating time is plotted in the inset of Fig. 2(d) as a function of the driving frequency. It can be seen that the heating time is a few orders of magnitude longer at the dynamical localization point in comparison to what is seen when the parameters are tuned away from it. This stems from the fact that driving at the dynamical localization point amounts to a suppression

of the hopping parameter leaving the other parameters unchanged [40, 79].

We now consider the effect of disorder on top of quasiperiodic driving and interactions. The interplay of hopping suppression, dynamical localization, and disorder results in a slow relaxation even in the ergodic phase. We maintain the strength of the disorder potential at $W = 1.0$, which in the undriven case, lies in the ergodic region where the auto-correlation function shows power-law decay and the transport is diffusive [60]. We plot the auto-correlation function and the entanglement entropy for Fibonacci driving in Fig. 2(b,e) for different driving frequencies and with the parameters tuned at the dynamical localization point. Although the undriven system lies in the ergodic regime, we see that the quasiperiodic drive slows down the dynamics and induces logarithmically slow relaxation of the auto-correlation function and a slow growth of the entanglement entropy. This is in contrast to earlier work where a logarithmic relaxation was observed in the many-body localized phase alone [45].

A comparison between the different quasiperiodic driving protocols, random driving and the case of no driving is shown in Fig. 2(c,f) for a fixed frequency $\omega = 8.0$. While for the undriven and the random driving cases, a fast relaxation is obtained, we note that quasiperiodic driving leads to logarithmic relaxation. It is also worth noting that the glassy phase has a longer lasting window

for Fibonacci driving in comparison to the Thue-Morse one. This could possibly be due to the additional frequency components in the Fourier spectrum of the Thue-Morse sequence [48, 49].

Summary and conclusions: To summarize, we study the dynamics of fermions in a disordered potential subjected to a time-dependent electric field taken from discrete quasiperiodic Fibonacci and Thue-Morse sequences. In the clean non-interacting case, we show that dynamical localization is possible with quasiperiodic driving and provide the conditions under which it can be seen. In the presence of disorder, we find that the quasiperiodic drive destroys Anderson localization but yields a slow relaxation where the growth of entanglement entropy is sub-linear. In the presence of many-body interactions, dynamical localization gets destroyed. However, turning on interactions in a system that is tuned at the dynamical localization point, we show that the heating can be suppressed significantly in comparison to the case where the parameters are tuned away from dynamical localization. Finally, exploiting the concept of dynamical localization and hopping suppression, we show that quasiperiodic driving induces slow logarithmic relaxation in the ergodic regime of an interacting system where the undriven system is known to relax very fast. Our work thus potentially provides ways to host non-equilibrium phases of matter, such as time quasi-crystals [45, 48] and also opens up the possibility of using quasiperiodic electric field driving to manipulate the properties of quantum systems in the same spirit as periodic electric field driving. In the future, it will be interesting to see how the presence of longer-range hopping or interaction affects dynamical localization and quantum transport in these systems. Additionally, it is worth exploring features like coherent/incoherent destruction of Wannier-Stark localization [26, 80] and super-Bloch oscillations [22, 28] in such driven systems.

ACKNOWLEDGMENTS

We are grateful to the High Performance Computing (HPC) facility at IISER Bhopal, where large-scale calculations in this project were run. We acknowledge QuSpin package [81, 82] for help in the numerical exact-diagonalization. V.T is grateful to DST-INSPIRE for her PhD fellowship. A.S acknowledges financial support from SERB via the grant (File Number: CRG/2019/003447), and from DST via the DST-INSPIRE Faculty Award [DST/INSPIRE/04/2014/002461].

* auditya@iiserb.ac.in

- [1] J. Eisert, M. Friesdorf, and C. Gogolin, Quantum many-body systems out of equilibrium, *Nature Physics* **11**, 124 (2015).
- [2] A. Haldar and A. Das, Dynamical many-body localization and delocalization in periodically driven closed quantum systems, *Annalen der Physik* **529**, 1600333 (2017).
- [3] B. Mukherjee, S. Nandy, A. Sen, D. Sen, and K. Sen-gupta, Collapse and revival of quantum many-body scars via floquet engineering, *Phys. Rev. B* **101**, 245107 (2020).
- [4] V. Khemani, A. Lazarides, R. Moessner, and S. L. Sondhi, Phase structure of driven quantum systems, *Phys. Rev. Lett.* **116**, 250401 (2016).
- [5] G. Casati and J. Ford, Stochastic behavior in classical and quantum hamiltonian systems **93**, 10.1007/BFB0021732 (1979).
- [6] G. Lemarié, J. Chabé, P. Szriftgiser, J. C. Garreau, B. Grémaud, and D. Delande, Observation of the anderson metal-insulator transition with atomic matter waves: Theory and experiment, *Phys. Rev. A* **80**, 043626 (2009).
- [7] D. R. Grempel, R. E. Prange, and S. Fishman, Quantum dynamics of a nonintegrable system, *Phys. Rev. A* **29**, 1639 (1984).
- [8] A. Haldar, D. Sen, R. Moessner, and A. Das, Dynamical freezing and scar points in strongly driven floquet matter: Resonance vs emergent conservation laws, *Phys. Rev. X* **11**, 021008 (2021).
- [9] T. Kitagawa, E. Berg, M. Rudner, and E. Demler, Topological characterization of periodically driven quantum systems, *Phys. Rev. B* **82**, 235114 (2010).
- [10] N. H. Lindner, G. Refael, and V. Galitski, Floquet topological insulator in semiconductor quantum wells, *Nature Physics* **7**, 490 (2011).
- [11] C. Fleckenstein and M. Bukov, Prethermalization and thermalization in periodically driven many-body systems away from the high-frequency limit, *Phys. Rev. B* **103**, L140302 (2021).
- [12] W. Beatrez, O. Janes, A. Akkiraju, A. Pillai, A. Oddo, P. Reshetikhin, E. Druga, M. McAllister, M. Elo, B. Gilbert, D. Suter, and A. Ajoy, Floquet prethermalization with lifetime exceeding 90 s in a bulk hyperpolarized solid, *Phys. Rev. Lett.* **127**, 170603 (2021).
- [13] S. A. Weidinger and M. Knap, Floquet prethermalization and regimes of heating in a periodically driven, interacting quantum system, *Scientific Reports* **7**, 45382 (2017).
- [14] A. Morningstar, M. Hauru, J. Beall, M. Ganahl, A. G. Lewis, V. Khemani, and G. Vidal, Simulation of quantum many-body dynamics with tensor processing units: Floquet prethermalization, *PRX Quantum* **3**, 020331 (2022).
- [15] D. A. Abanin, W. De Roeck, W. W. Ho, and F. m. c. Huveneers, Effective hamiltonians, prethermalization, and slow energy absorption in periodically driven many-body systems, *Phys. Rev. B* **95**, 014112 (2017).
- [16] D. V. Else, B. Bauer, and C. Nayak, Floquet time crystals, *Phys. Rev. Lett.* **117**, 090402 (2016).
- [17] B. Huang, Y.-H. Wu, and W. V. Liu, Clean floquet time crystals: Models and realizations in cold atoms, *Phys. Rev. Lett.* **120**, 110603 (2018).
- [18] N. Y. Yao, A. C. Potter, I.-D. Potirniche, and A. Vishwanath, Discrete time crystals: Rigidity, criticality, and realizations, *Phys. Rev. Lett.* **118**, 030401 (2017).
- [19] J. Zhang, P. W. Hess, A. Kyprianidis, P. Becker, A. Lee, J. Smith, G. Pagano, I.-D. Potirniche, A. C. Potter, A. Vishwanath, N. Y. Yao, and C. Monroe, Observation of a discrete time crystal, *Nature* **543**, 217 (2017).

- [20] D. Dunlap and V. Kenkre, Dynamic localization of a particle in an electric field viewed in momentum space: Connection with bloch oscillations, *Physics Letters A* **127**, 438 (1988).
- [21] D. H. Dunlap and V. M. Kenkre, Dynamic localization of a charged particle moving under the influence of an electric field, *Phys. Rev. B* **34**, 3625 (1986).
- [22] D. S. Bhakuni and A. Sharma, Characteristic length scales from entanglement dynamics in electric-field-driven tight-binding chains, *Phys. Rev. B* **98**, 045408 (2018).
- [23] A. Eckardt, M. Holthaus, H. Lignier, A. Zenesini, D. Ciampini, O. Morsch, and E. Arimondo, Exploring dynamic localization with a bose-einstein condensate, *Phys. Rev. A* **79**, 013611 (2009).
- [24] H. Lignier, C. Sias, D. Ciampini, Y. Singh, A. Zenesini, O. Morsch, and E. Arimondo, Dynamical control of matter-wave tunneling in periodic potentials, *Phys. Rev. Lett.* **99**, 220403 (2007).
- [25] M. Holthaus, G. H. Ristow, and D. W. Hone, Random lattices in combined a.c. and d.c. electric fields: Anderson vs. wannier-stark localization, *Europhysics Letters (EPL)* **32**, 241 (1995).
- [26] M. Holthaus, G. H. Ristow, and D. W. Hone, ac-field-controlled anderson localization in disordered semiconductor superlattices, *Phys. Rev. Lett.* **75**, 3914 (1995).
- [27] V. Tiwari, D. S. Bhakuni, and A. Sharma, Noise-induced dynamical localization and delocalization, *Phys. Rev. B* **105**, 165114 (2022).
- [28] D. S. Bhakuni, R. Nehra, and A. Sharma, Drive-induced many-body localization and coherent destruction of stark many-body localization, *Phys. Rev. B* **102**, 024201 (2020).
- [29] S. Longhi and G. Della Valle, Correlated super-bloch oscillations, *Phys. Rev. B* **86**, 075143 (2012).
- [30] K. Kudo and T. S. Monteiro, Theoretical analysis of super-bloch oscillations, *Phys. Rev. A* **83**, 053627 (2011).
- [31] M. Schulz, C. A. Hooley, R. Moessner, and F. Pollmann, Stark many-body localization, *Phys. Rev. Lett.* **122**, 040606 (2019).
- [32] D. S. Bhakuni and A. Sharma, Entanglement and thermodynamic entropy in a clean many-body-localized system, *Journal of Physics: Condensed Matter* **32**, 255603 (2020).
- [33] W. Morong, F. Liu, P. Becker, K. S. Collins, L. Feng, A. Kyprianidis, G. Pagano, T. You, A. V. Gorshkov, and C. Monroe, Observation of stark many-body localization without disorder, *Nature* **599**, 393 (2021).
- [34] Q. Guo, C. Cheng, H. Li, S. Xu, P. Zhang, Z. Wang, C. Song, W. Liu, W. Ren, H. Dong, R. Mondaini, and H. Wang, Stark many-body localization on a superconducting quantum processor (2020), [arXiv:2011.13895 \[quant-ph\]](https://arxiv.org/abs/2011.13895).
- [35] S. R. Taylor, M. Schulz, F. Pollmann, and R. Moessner, Experimental probes of stark many-body localization, *Phys. Rev. B* **102**, 054206 (2020).
- [36] E. van Nieuwenburg, Y. Baum, and G. Refael, From bloch oscillations to many-body localization in clean interacting systems, *Proceedings of the National Academy of Sciences* **116**, 9269 (2019), <https://www.pnas.org/doi/pdf/10.1073/pnas.1819316116>.
- [37] G. Zisling, D. M. Kennes, and Y. Bar Lev, Transport in stark many-body localized systems, *Phys. Rev. B* **105**, L140201 (2022).
- [38] E. V. H. Doggen, I. V. Gornyi, and D. G. Polyakov, Stark many-body localization: Evidence for hilbert-space shattering, *Phys. Rev. B* **103**, L100202 (2021).
- [39] P. Ribeiro, A. Lazarides, and M. Haque, Many-body quantum dynamics of initially trapped systems due to a stark potential: Thermalization versus bloch oscillations, *Phys. Rev. Lett.* **124**, 110603 (2020).
- [40] E. Bairey, G. Refael, and N. H. Lindner, Driving induced many-body localization, *Phys. Rev. B* **96**, 020201 (2017).
- [41] A. Kshetrimayum, J. Eisert, and D. M. Kennes, Stark time crystals: Symmetry breaking in space and time, *Phys. Rev. B* **102**, 195116 (2020).
- [42] S. Liu, S.-X. Zhang, C.-Y. Hsieh, S. Zhang, and H. Yao, Discrete time crystal enabled by stark many-body localization (2022).
- [43] A. Verdeny, J. Puig, and F. Mintert, Quasi-periodically driven quantum systems, *Zeitschrift für Naturforschung A* **71**, 897 (2016).
- [44] S. Nandy, A. Sen, and D. Sen, Aperiodically driven integrable systems and their emergent steady states, *Phys. Rev. X* **7**, 031034 (2017).
- [45] P. T. Dumitrescu, R. Vasseur, and A. C. Potter, Logarithmically slow relaxation in quasiperiodically driven random spin chains, *Phys. Rev. Lett.* **120**, 070602 (2018).
- [46] K. Giergiel, A. Kuroś, and K. Sacha, Discrete time quasicrystals, *Phys. Rev. B* **99**, 220303 (2019).
- [47] S. Ray, S. Sinha, and D. Sen, Dynamics of quasiperiodically driven spin systems, *Phys. Rev. E* **100**, 052129 (2019).
- [48] H. Zhao, F. Mintert, R. Moessner, and J. Knolle, Random multipolar driving: Tunably slow heating through spectral engineering, *Phys. Rev. Lett.* **126**, 040601 (2021).
- [49] S. Nandy, A. Sen, and D. Sen, Steady states of a quasiperiodically driven integrable system, *Phys. Rev. B* **98**, 245144 (2018).
- [50] S. Maity, U. Bhattacharya, A. Dutta, and D. Sen, Fibonacci steady states in a driven integrable quantum system, *Phys. Rev. B* **99**, 020306 (2019).
- [51] D. M. Long, P. J. D. Crowley, and A. Chandran, Many-body localization with quasiperiodic driving (2021).
- [52] H. Zhao, F. Mintert, J. Knolle, and R. Moessner, Localization persisting under aperiodic driving (2021).
- [53] G. Abal, R. Donangelo, A. Romanelli, A. C. Sicardi Schifino, and R. Siri, Dynamical localization in quasiperiodic driven systems, *Phys. Rev. E* **65**, 046236 (2002).
- [54] S. Bhattacharjee, S. Bandyopadhyay, and A. Dutta, Quasi-localization dynamics in a fibonacci quantum rotor (2021).
- [55] T. Martin, I. Martin, and K. Agarwal, Effect of quasiperiodic and random noise on many-body dynamical decoupling protocols, *Phys. Rev. B* **106**, 134306 (2022).
- [56] D. V. Else, W. W. Ho, and P. T. Dumitrescu, Long-lived interacting phases of matter protected by multiple time-translation symmetries in quasiperiodically driven systems, *Phys. Rev. X* **10**, 021032 (2020).
- [57] B. Mukherjee, A. Sen, D. Sen, and K. Sengupta, Restoring coherence via aperiodic drives in a many-body quantum system, *Phys. Rev. B* **102**, 014301 (2020).
- [58] P. T. Dumitrescu, J. G. Bohnet, J. P. Gaebler, A. Hankin, D. Hayes, A. Kumar, B. Neyenhuis, R. Vasseur, and A. C. Potter, Dynamical topological phase realized in a trapped-ion quantum simulator, *Nature* **607**, 463 (2022).

- [59] P. W. Anderson, Absence of diffusion in certain random lattices, *Physical review* **109**, 1492 (1958).
- [60] K. Agarwal, S. Gopalakrishnan, M. Knap, M. Müller, and E. Demler, Anomalous diffusion and griffiths effects near the many-body localization transition, *Phys. Rev. Lett.* **114**, 160401 (2015).
- [61] E. Abrahams, P. W. Anderson, D. C. Licciardello, and T. V. Ramakrishnan, Scaling theory of localization: Absence of quantum diffusion in two dimensions, *Phys. Rev. Lett.* **42**, 673 (1979).
- [62] D. J. Luitz, N. Laflorencie, and F. Alet, Many-body localization edge in the random-field heisenberg chain, *Phys. Rev. B* **91**, 081103 (2015).
- [63] A. Pal and D. A. Huse, Many-body localization phase transition, *Phys. Rev. B* **82**, 174411 (2010).
- [64] W. De Roeck and F. m. c. Huveneers, Stability and instability towards delocalization in many-body localization systems, *Phys. Rev. B* **95**, 155129 (2017).
- [65] D. Abanin, J. Bardarson, G. De Tomasi, S. Gopalakrishnan, V. Khemani, S. Parameswaran, F. Pollmann, A. Potter, M. Serbyn, and R. Vasseur, Distinguishing localization from chaos: Challenges in finite-size systems, *Annals of Physics* **427**, 168415 (2021).
- [66] A. Morningstar, L. Colmenarez, V. Khemani, D. J. Luitz, and D. A. Huse, Avalanches and many-body resonances in many-body localized systems, *Phys. Rev. B* **105**, 174205 (2022).
- [67] T. Hartmann, F. Keck, H. J. Korsch, and S. Mossmann, Dynamics of bloch oscillations, *New Journal of Physics* **6**, 2 (2004).
- [68] B. C. Hall, Lie groups, lie algebras, and representations, in *Quantum Theory for Mathematicians* (Springer New York, New York, NY, 2013) pp. 333–366.
- [69] M. A. Nielsen and I. L. Chuang, *Quantum Computation and Quantum Information: 10th Anniversary Edition* (Cambridge University Press, 2010).
- [70] I. Peschel, Calculation of reduced density matrices from correlation functions, *Journal of Physics A: Mathematical and General* **36**, L205 (2003).
- [71] N. Roy and A. Sharma, Entanglement contour perspective for “strong area-law violation” in a disordered long-range hopping model, *Phys. Rev. B* **97**, 125116 (2018).
- [72] W. Zhang and S. E. Ulloa, ac-field-controlled localization-delocalization transition in a one-dimensional disordered system, *Phys. Rev. B* **74**, 115304 (2006).
- [73] D. N. Page, Average entropy of a subsystem, *Phys. Rev. Lett.* **71**, 1291 (1993).
- [74] D. S. Bhakuni and A. Sharma, Stability of electric field driven many-body localization in an interacting long-range hopping model, *Phys. Rev. B* **102**, 085133 (2020).
- [75] T. L. M. Lezama, S. Bera, and J. H. Bardarson, Apparent slow dynamics in the ergodic phase of a driven many-body localized system without extensive conserved quantities, *Phys. Rev. B* **99**, 161106 (2019).
- [76] Y. Bar Lev, G. Cohen, and D. R. Reichman, Absence of diffusion in an interacting system of spinless fermions on a one-dimensional disordered lattice, *Phys. Rev. Lett.* **114**, 100601 (2015).
- [77] D. J. Luitz and Y. B. Lev, The ergodic side of the many-body localization transition, *Annalen der Physik* **529**, 1600350 (2017).
- [78] D. S. Bhakuni, L. F. Santos, and Y. B. Lev, Suppression of heating by long-range interactions in periodically driven spin chains, *Phys. Rev. B* **104**, L140301 (2021).
- [79] D. J. Luitz, Y. B. Lev, and A. Lazarides, Absence of dynamical localization in interacting driven systems, *SciPost Phys.* **3**, 029 (2017).
- [80] D. S. Bhakuni, S. Dattagupta, and A. Sharma, Effect of noise on bloch oscillations and wannier-stark localization, *Phys. Rev. B* **99**, 155149 (2019).
- [81] P. Weinberg and M. Bukov, QuSpin: a Python package for dynamics and exact diagonalisation of quantum many body systems part I: spin chains, *SciPost Phys.* **2**, 003 (2017).
- [82] P. Weinberg and M. Bukov, QuSpin: a Python package for dynamics and exact diagonalisation of quantum many body systems. Part II: bosons, fermions and higher spins, *SciPost Phys.* **7**, 020 (2019).

Supplementary material: Quasiperiodic driving induced slow relaxation in interacting thermalizing systems

Vatsana Tiwari,¹ Devendra Singh Bhakuni,² and Auditya Sharma^{1,*}

¹*Department of Physics, Indian Institute of Science Education and Research, Bhopal, India*

²*Department of Physics, Ben-Gurion University of the Negev, Beer-Sheva 84105, Israel*

I. FIBONACCI DRIVING

A. Non-interacting Limit

For the Fibonacci sequence, we define the unitary operators $U_0 = e^{-iTH_A}$, and $U_1 = e^{-iTH_B}$ corresponding to the electric field $\pm F$ respectively and generate the subsequent evolution according to the Fibonacci sequence [1]:

$$U_n = U_{n-2}U_{n-1}, \quad n \geq 2. \quad (1)$$

For simplicity, let us first study the stroboscopic unitary operator defined at Fibonacci level $m = 2$ with two pulses A and B as

$$U(N=2) = U_B U_A = \exp(-iTH_B) \exp(-iTH_A) \quad (2)$$

Using the BCH formula [2]:

$$e^X e^Y = \exp \left[X + Y + \frac{1}{2}[X, Y] + f([X, Y, [\dots]]) + \dots \right], \quad (3)$$

we get

$$U(N=2) = U_B U_A \equiv \exp(-2iTH_{BA}^{\text{eff}}), \quad (4)$$

where

$$H_{BA}^{\text{eff}} = \Delta_f \left[\hat{K} e^{-i\frac{FT}{2}} + \hat{K}^\dagger e^{i\frac{FT}{2}} \right]. \quad (5)$$

Here, $\Delta_f = \frac{-\Delta}{4} \frac{\sin \frac{FT}{2}}{\frac{FT}{2}}$, $T = \frac{2\pi}{\omega}$. Thus, we observe from Eq.(8) that the coefficients of \hat{K} and \hat{K}^\dagger get renormalized. By tuning the amplitude of the drive at $F/\omega = n(n \in \mathbb{Z})$, the effective hopping term vanishes, and $U(N=2)$ (Eq. (2)) takes the form of an identity operator which implies that any state will return to its initial position after this time period and hence will be dynamically localized. Next, let us consider the case of $m = 4$, where we have 5 pulses: A, B, A, A, B . We can define the stroboscopic unitary operator as a product of U_A s and U_B s:

$$U(N=5) = U_B U_A U_A U_B U_A. \quad (6)$$

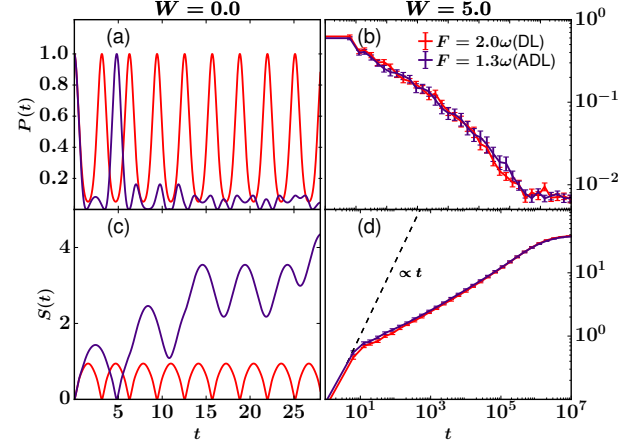


Figure 1. (a,b): Dynamics of return probability $P(t)$ at dynamical localization point ($F = n\omega$) and away from dynamical localization ($F \neq n\omega$) for Fibonacci driven clean ($W = 0.0$) and disordered non-interacting system. (c,d): Entanglement entropy $S(t)$ for Fibonacci driven clean ($W = 0.0$) and disordered ($W = 5.0$) non-interacting system at dynamical localization point ($F = n\omega$) and away from dynamical localization ($F \neq n\omega$). The other parameters are $\Delta = 4.0, \omega = 1.0, L = 200$. The time discretization for our numerics is $\Delta t = 0.001$. For the disordered case, we have averaged over 100 realizations of disorder. In (d), the (linear) black dashed line indicates the ballistic growth of entanglement entropy ($S(t) \propto t$).

It is useful to pair up consecutive unitary operators associated with different types of pulses (A and B); we thus define the Floquet unitary operators U_C and $U_{C'}$:

$$U_C = U_B U_A \equiv \exp(-2iTH_{BA}^{\text{eff}}), \quad (7)$$

$$H_{BA}^{\text{eff}} = \Delta_f \left[\hat{K} e^{-i\frac{FT}{2}} + \hat{K}^\dagger e^{i\frac{FT}{2}} \right], \quad (8)$$

$$U_{C'} = U_A U_B \equiv \exp(-2iTH_{AB}^{\text{eff}}), \quad (9)$$

$$H_{AB}^{\text{eff}} = \Delta_f \left[\hat{K} e^{i\frac{FT}{2}} + \hat{K}^\dagger e^{-i\frac{FT}{2}} \right]. \quad (10)$$

Using Eq. (7), and (9), we can rewrite Eq. (6) as:

$$\begin{aligned} U(N=5) &= U_C U_{C'} U_A, \\ &\equiv \exp(-2iTH_{BA}^{\text{eff}}) \exp(-2iTH_{AB}^{\text{eff}}) U_A. \end{aligned} \quad (11)$$

It is clear from Eq. (8) and Eq. (10) that at $F = n\omega$, both U_C and $U_{C'}$ become the identity operator and the

* auditya@iiserb.ac.in

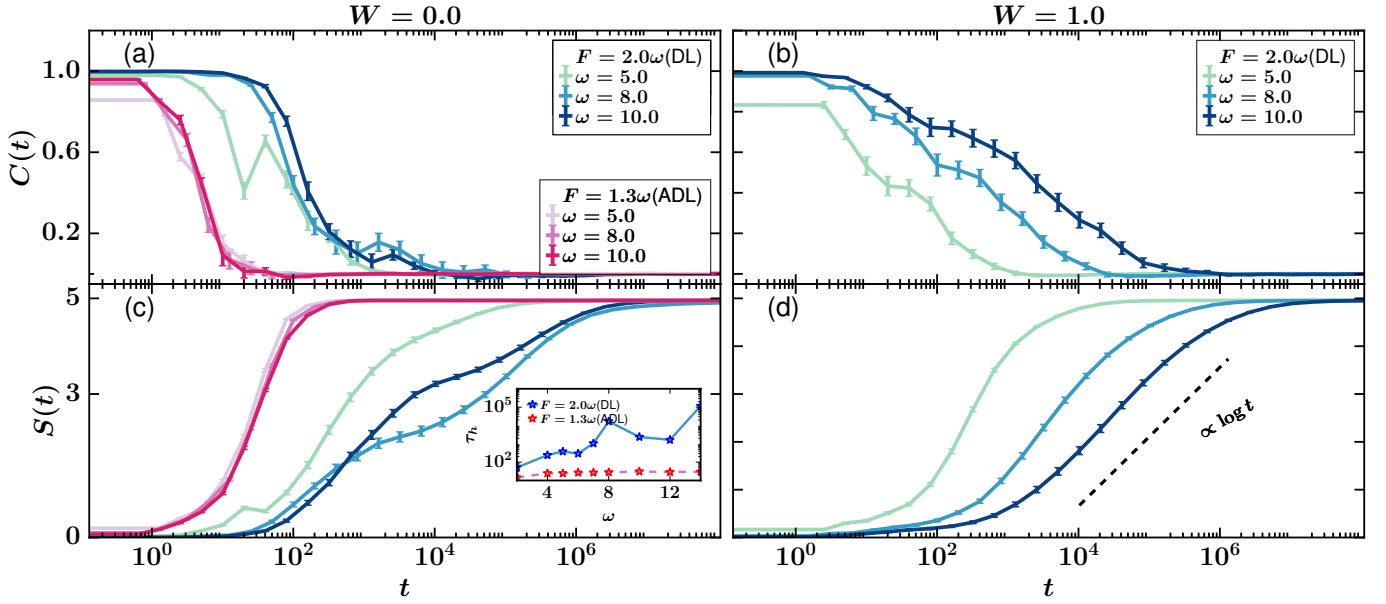


Figure 2. (a,c): Auto-correlation $C(t)$ and half chain entanglement entropy $S(t)$ for Thouless-Morse driven clean ($W = 0.0$) interacting system. In (a) and (c), the plots in pink shades correspond to the parameters being tuned away from dynamical localization (ADL) ($F = 1.3\omega$), and blue shade plots correspond to the parameters being tuned at dynamical localization (DL) ($F = 2.0\omega$). Inset(c): Heating time τ_h vs frequency ω . (b, d): $C(t)$ and $S(t)$ for Thouless-Morse driven disordered ($W = 1.0$) interacting system. We have averaged over 100 disorder realizations. In (d), the black dashed line is drawn to show logarithmic growth of entanglement entropy ($S(t) \propto \log t$) for $\omega = 10$. The other system parameters are $\Delta = 4.0, U = 1.0, F = 2.0\omega$, and system size $L = 16$.

clean (Fig. 2(a,c)) and disordered interacting system (Fig. 2(b,d)). For the clean system, the dynamics for $F/\omega = 1.3$ (away from dynamical localization) quickly approaches the Page value (pink shade curves), whereas for $F/\omega = 2.0$, the system relaxes to the infinite temperature state very slowly (blue shade curves). To distinguish the dynamics of the system at the dynamical localization (DL) point and away from the dynamical localization (ADL) point, we plot the heating time as a function of frequency (τ_h vs ω) in the inset of Fig. 2(c) for $F = 2.0\omega$ (DL), and $F = 1.3\omega$ (ADL). It clearly shows that the significant suppression of hopping strength at

DL leads to a slow heating of the system. In contrast, the system quickly reaches a featureless infinite temperature state on tuning the parameters away from DL.

In Fig. 2(b,d), we focus on the ergodic side of the disordered system by fixing the disorder strength to be $W = 1.0$, and drive the system at the dynamical localization point $F/\omega = 2.0$. $C(t)$ and $S(t)$ exhibit the same behavior as shown in the Fibonacci driven case in the main Letter. The entanglement entropy attains the Page value (corresponding to the infinite temperature state) logarithmically slowly ($S(t) \propto \log t$) (Fig. 2(d)), indicating glassy dynamics.

-
- [1] S. Maity, U. Bhattacharya, A. Dutta, and D. Sen, Fibonacci steady states in a driven integrable quantum system, *Phys. Rev. B* **99**, 020306 (2019).
 [2] B. C. Hall, Lie groups, lie algebras, and representations,

- in *Quantum Theory for Mathematicians* (Springer New York, New York, NY, 2013) pp. 333–366.
 [3] H. Zhao, F. Mintert, R. Moessner, and J. Knolle, Random multipolar driving: Tunably slow heating through spectral engineering, *Phys. Rev. Lett.* **126**, 040601 (2021).